

# Simultaneous identification of *EGFR*, *KRAS*, *ERBB2*, and *TP53* mutations in patients with non-small cell lung cancer by machine learning-derived three-dimensional radiomics

Tiening Zhang<sup>1</sup>, Zhihan Xu<sup>2</sup>, Guixue Liu<sup>3</sup>, Beibei Jiang<sup>3</sup>, Geertruida H. de Bock<sup>4</sup>, Harry JM Groen<sup>5</sup>, Rozemarijn Vliegthart<sup>6</sup>, Xueqian Xie<sup>3</sup>

**Table S1.** CT acquisition protocols and image reconstruction parameters

| CT scanner            | Siemens Somatom Force   | GE Revolution        |
|-----------------------|-------------------------|----------------------|
| Acquisition mode      | Helical                 | Helical              |
| Tube voltage, kV      | 100                     | 120                  |
| Tube current, mA      | 130 (quality reference) | 100-400 (smart mode) |
| Collimation, mm       | 192×0.6                 | 256×0.625            |
| Pitch                 | 1.2                     | 0.984                |
| Rotation time, ms     | 500                     | 500                  |
| Reconstruction kernel | Br44                    | Standard             |
| Field of view, mm     | 325                     | 325                  |
| Slice thickness, mm   | 0.6                     | 0.625                |
| Slice increment, mm   | 0.6                     | 0.625                |
| Radiation dose, mGy   | ≈4.52                   | ≈5.20                |

**Table S2.** Variation of *EGFR*, *KRAS*, *ERBB2*, and *TP53* mutations

| <i>EGFR</i>   |        | <i>KRAS</i>   |        | <i>ERBB2</i>  |        | <i>TP53</i>   |        |
|---------------|--------|---------------|--------|---------------|--------|---------------|--------|
| Mutation site | Number | Mutation site | Number | Mutation site | Number | Mutation site | Number |
| Exon-5        | 2      | Exon-2        | 10     | Exon-21       | 2      | Exon-4        | 7      |
| Exon-18       | 3      | Exon-3        | 3      | Exon-12       | 1      | Exon-3        | 2      |
| Exon-19       | 25     | 12P12.1       | 2      | Exon-20       | 6      | Exon-5        | 11     |
| Exon-20       | 7      |               |        | Exon-17       | 1      | Exon-6        | 9      |
| Exon-21       | 24     |               |        | Exon-19       | 1      | Exon-7        | 11     |
| Exon18-25     | 1      |               |        | Exon-22       | 1      | Exon-8        | 12     |
| 7P11.2        | 3      |               |        | 17Q12         | 1      | Exon-9        | 3      |
|               |        |               |        |               |        | C.1045G>T     | 1      |
|               |        |               |        |               |        | c.375+2T>A    | 1      |
|               |        |               |        |               |        | P.ARG248PR    | 1      |
|               |        |               |        |               |        | O             | 1      |
|               |        |               |        |               |        | C.602T>A      | 1      |
|               |        |               |        |               |        | P.LEU201*     | 1      |
| Total         | 65     | Total         | 15     | Total         | 13     | Total         | 60     |

*EGFR*= epidermal growth factor receptor; *KRAS*= Kirsten rat sarcoma viral oncogene; *ERBB2*= Erb-B2 receptor tyrosine kinase 2; *TP53*= tumor protein 53

*EGFR* Exon-5: p.A138V, p.V173M

Exon-18: p.G719A, p.E709A

Exon-19: C.2235\_2249, C.2236\_2250, C.2239\_2255, C.2237\_2255, C.2240\_2254, C.2239\_2248, p.E746\_A750, p.L858R, p.E746\_A750, p.E746\_S752

Exon-20: p.N771\_p 772, p.T790M, p.S768\_D770, p.H773\_V774

Exon-21: p.L858R, p.L861Q, p.L858R

*KRAS* Exon-2: p.G12A, p.G12C, p.G12D, p.G12V, p.G13C

Exon-3: p.Q61H

*ERBB2* Exon-21: p.L858R

Exon-12: C.1397C>T

Exon-20: C.2332, p.GLY778, C.2313, p.ALA775, p.Y772, p.G778,

Exon-17: p.V659E

Exon19: p.I767M

Exon22: p.R896G

*TP53* Exon-3: C.96+1G>T,

Exon-4: p.S106Afs\*17, p.E68Dfs\*51, p.L43\*, p.P72Rfs\*41, C.375+1G>T, C.202G>T, p.GLU68\*

Exon-5: p.E180K, p.H179R, p.V157F, p.R158L, p.V173L, p.H179R, p.Q167\*, p.A159V, p.G154V, p.R158G  
 Exon-6: p.L194R, p.Y220S, p.E204\*, p.H193Y, p.Q192\*, p.R213L, p.S215G, p.V216M, C.569C>T, p.S241F, C.569C>T  
 Exon-7: p.R248G, p.G245S, p.R248W, C.673-2A>T, p.N235D, p.G244V, p.G244D, p.L257R, p.Y220C, p.M246V, C.736A>G,  
 p.GLY245FS  
 Exon-8: p.I767M, p.C277F, P.R273C, p.R280K, p.GLU294FS, p.V272L, p.G266E, p.P278H, p.R280T, p.G266V  
 Exon-9: p.R896G, C.920-1G>A, p.E326Dfs\*19

**Table S3.** Finally selected features with a non-zero coefficient after the least absolute shrinkage and selection operator (LASSO) selection

| Model                                       | EnrolledFeature  | Feature Type | Spearman's correlation coefficient | Coefficient (LASSO Logistic) |
|---|--|--------------|------------------------------------|------------------------------|
| EGFR  | original_shape_Maximum2DDiameterSlice                      | Shape        | 0.992885                           | 0.462044                     |
|   | square_glcm_DifferenceAverage                              | Texture      | 0.88451                            | 2.701276                     |
|   | square_glcm_JointEnergy                                    | Texture      | 0.918446                           | -0.3922                      |
|   | square_ngtdm_Busyness                                      | Texture      | 0.871921                           | 0.127518                     |
|   | square_ngtdm_Complexity                                    | Texture      | 0.802408                           | -0.09055                     |
|   | squareroot_firstorder_90Percentile                         | First-order  | 0.94855                            | 2.658891                     |
|   | squareroot_glrmlm_RunLengthNonUniformityNormalized         | Texture      | 0.935961                           | -0.36438                     |
|   | wavelet.LHH_glrmlm_ShortRunEmphasis                        | Texture      | 0.819376                           | -0.44897                     |
|   | wavelet.LHL_firstorder_10Percentile                        | First-order  | 0.901478                           | 0.137372                     |
|   | wavelet.LHL_firstorder_TotalEnergy                         | First-order  | 0.922824                           | -0.42447                     |
|   | wavelet.LLH_firstorder_90Percentile                        | First-order  | 0.847291                           | -0.06422                     |
|   | wavelet.LLH_glrmlm_LongRunEmphasis                         | Texture      | 0.939245                           | -0.44264                     |
| log.sigma.0.5.mm.3D_glszm_GrayLevelVariance | Texture  | 0.829228     | -0.56618                           |                              |
| ERBB2                                       | original_glcm_Contrast                                     | Texture      | 0.874658                           | -1.16287                     |
|   | logarithm_glrmlm_GrayLevelNonUniformity                    | Texture      | 0.996716                           | 0.161683                     |
|   | exponential_gldm_DependenceNonUniformity                   | Texture      | 0.992337                           | 1.925881                     |
|   | exponential_gldm_GrayLevelVariance                         | Texture      | 0.995751                           | 0.360805                     |
|   | exponential_ngtdm_Complexity                               | Texture      | 0.998938                           | -0.13601                     |
|   | wavelet.LHH_gldm_DependenceNonUniformity                   | Texture      | 0.983032                           | -1.42815                     |
|   | wavelet.LHL_gldm_GrayLevelVariance                         | Texture      | 0.827586                           | 0.245614                     |
|   | wavelet.LLH_glrmlm_LongRunEmphasis                         | Texture      | 0.939245                           | -1.07933                     |
|   | log.sigma.0.5.mm.3D_gldm_DependenceNonUniformityNormalized | Texture      | 0.918446                           | 0.802951                     |

|                                       |  |             |          |          |
|---------------------------------------|--|-------------|----------|----------|
|                                       | log.sigma.1.5.mm.3D_glrIm_GrayLevelVariance                | Texture     | 0.893815 | 0.143292 |
|                                       | log.sigma.2.5.mm.3D_glcM_Imc1                              | Texture     | 0.975917 | 2.884485 |
|                                       | log.sigma.2.5.mm.3D_glcM_Imc2                              | Texture     | 0.896552 | 1.172461 |
|                                       | log.sigma.2.5.mm.3D_glszm_SizeZoneNonUniformity            | Texture     | 0.95676  | 0.262752 |
|                                       | log.sigma.4.5.mm.3D_firstorder_Entropy                     | First-order | 0.888889 | -0.36531 |
|                                       | log.sigma.4.5.mm.3D_gldm_DependenceNonUniformity           | Texture     | 0.992337 | -0.36871 |
|                                       | log.sigma.4.5.mm.3D_ngtdm_Coarseness                       | Texture     | 0.992885 | -2.55691 |
| KRAS                                  | squareroot_glcM_Idn  | Texture     | 0.935961 | 0.595243 |
|                                       | wavelet.LHL_glcM_DifferenceVariance                        | Texture     | 0.841817 | -0.02693 |
|                                       | wavelet.LLH_firstorder_RobustMeanAbsoluteDeviation         | First-order | 0.949097 | -0.30775 |
|                                       | log.sigma.0.5.mm.3D_glcM_InverseVariance                   | Texture     | 0.914067 | 0.105427 |
|                                       | log.sigma.1.5.mm.3D_firstorder_Mean                        | First-order | 0.993432 | 0.353714 |
|                                       | log.sigma.1.5.mm.3D_glrIm_RunVariance                      | Texture     | 0.992885 | -0.065   |
|                                       | log.sigma.1.5.mm.3D_glszm_LargeAreaLowGrayLevelEmphasis    | Texture     | 0.97318  | -0.03965 |
|                                       | log.sigma.1.5.mm.3D_glszm_SizeZoneNonUniformity            | Texture     | 0.955665 | 0.25912  |
|                                       | log.sigma.2.5.mm.3D_glcM_JointEntropy                      | Texture     | 0.966612 | 0.70026  |
|                                       | log.sigma.2.5.mm.3D_gldm_DependenceEntropy                 | Texture     | 0.915161 | -0.23615 |
|                                       | log.sigma.3.5.mm.3D_firstorder_RobustMeanAbsoluteDeviation | First-order | 0.840722 | -0.07761 |
|                                       | log.sigma.3.5.mm.3D_glcM_ClusterShade                      | Texture     | 0.962233 | 0.315677 |
|                                       | log.sigma.3.5.mm.3D_gldm_DependenceVariance                | Texture     | 0.984674 | -0.8243  |
|                                       | log.sigma.4.5.mm.3D_glcM_ClusterProminence                 | Texture     | 0.872469 | -0.53991 |
| TP53                                  | squareroot_glcM_Idn  | Texture     | 0.935961 | -0.7443  |
|                                       | wavelet.LHH_gldm_SmallDependenceEmphasis                   | Texture     | 0.83908  | -0.49639 |
|                                       | wavelet.LHL_glcM_DifferenceEntropy                         | Texture     | 0.863164 | -0.37893 |
|                                       | wavelet.LHL_glcM_DifferenceVariance                        | Texture     | 0.841817 | 0.10981  |
|                                       | wavelet.LLH_firstorder_RobustMeanAbsoluteDeviation         | First-order | 0.949097 | -1.21147 |
|                                       | log.sigma.0.5.mm.3D_glcM_InverseVariance                   | Texture     | 0.914067 | -0.89589 |
|                                       | log.sigma.1.5.mm.3D_firstorder_Mean                        | First-order | 0.993432 | -0.10977 |
|                                       | log.sigma.1.5.mm.3D_glszm_LargeAreaLowGrayLevelEmphasis    | Texture     | 0.97318  | -0.46992 |
|                                       | log.sigma.1.5.mm.3D_glszm_SizeZoneNonUniformity            | Texture     | 0.955665 | 0.144011 |
|                                       | log.sigma.2.5.mm.3D_gldm_DependenceEntropy                 | Texture     | 0.915161 | -0.191   |
|                                       | log.sigma.2.5.mm.3D_gldm_LowGrayLevelEmphasis              | Texture     | 0.975917 | -0.31674 |
|                                       | log.sigma.3.5.mm.3D_firstorder_RobustMeanAbsoluteDeviation | First-order | 0.840722 | 0.026772 |
| log.sigma.3.5.mm.3D_glcM_ClusterShade | Texture  | 0.962233    | 0.102195 |          |

|  |  |         |          |          |
|--|--|---------|----------|----------|
|  | log.sigma.3.5.mm.3D_gldm_DependenceVariance              | Texture | 0.984674 | -0.38159 |
|  | log.sigma.3.5.mm.3D_glrIm_LongRunHighGrayLevelEmphasis   | Texture | 0.990148 | 0.478267 |
|  | log.sigma.3.5.mm.3D_glszm_LargeAreaHighGrayLevelEmphasis | Texture | 0.992885 | 0.40209  |
|  | log.sigma.4.5.mm.3D_glcm_ClusterProminence               | Texture | 0.872469 | -0.1152  |

**Table S4.** Association between clinical factors and the presence of *EGFR*, *KRAS*, *ERBB2*, and *TP53* mutations

|                      | Total    | <i>EGFR</i>  |               |         | <i>KRAS</i>  |               |         | <i>ERBB2</i> |               |         | <i>TP53</i>  |               |         |
|----------------------|----------|--------------|---------------|---------|--------------|---------------|---------|--------------|---------------|---------|--------------|---------------|---------|
|                      |          | Wildtyp<br>e | Muta-<br>tion | P Value | Wildtyp<br>e | Muta-<br>tion | P Value | Wildtyp<br>e | Muta-<br>tion | P Value | Wildtyp<br>e | Muta-<br>tion | P Value |
| Number               | 134      | 69           | 65            |         | 119          | 15            |         | 121          | 13            |         | 74           | 60            |         |
| Age, years           | 63.6±8.9 | 64.1±9.5     | 62.7±10.7     | 0.411   | 63.2±10.4    | 64.7±7.6      | 0.608   | 60.4±10.1    | 66.5±10.2     | 0.251   | 60.9±10.1    | 66.4±9.3      | 0.001*  |
| Sex                  |          |              |               | 0.001*  |              |               | 0.036*  |              |               | 0.221   |              |               | 0.008*  |
| Female, <i>n</i>     | 56       | 19           | 37            |         | 54           | 2             |         | 49           | 8             |         | 35           | 21            |         |
| Male, <i>n</i>       | 78       | 50           | 28            |         | 65           | 13            |         | 73           | 5             |         | 39           | 39            |         |
| cT stage             |          |              |               | 0.813   |              |               | 0.602   |              |               | 0.044*  |              |               | 0.102   |
| 1, <i>n</i>          | 35       | 17           | 18            |         | 30           | 5             |         | 32           | 3             |         | 23           | 12            |         |
| 2, <i>n</i>          | 42       | 24           | 18            |         | 37           | 5             |         | 40           | 2             |         | 22           | 20            |         |
| 3, <i>n</i>          | 26       | 12           | 14            |         | 25           | 1             |         | 25           | 1             |         | 17           | 9             |         |
| 4, <i>n</i>          | 31       | 16           | 15            |         | 27           | 4             |         | 24           | 7             |         | 12           | 19            |         |
| cN stage             |          |              |               | 0.873   |              |               | 0.850   |              |               | 0.956   |              |               | 0.336   |
| 0, <i>n</i>          | 26       | 13           | 13            |         | 24           | 2             |         | 23           | 3             |         | 18           | 8             |         |
| 1, <i>n</i>          | 17       | 10           | 7             |         | 15           | 2             |         | 15           | 2             |         | 8            | 9             |         |
| 2, <i>n</i>          | 65       | 34           | 31            |         | 58           | 7             |         | 59           | 6             |         | 36           | 29            |         |
| 3, <i>n</i>          | 26       | 12           | 14            |         | 22           | 4             |         | 24           | 2             |         | 12           | 14            |         |
| cM stage             |          |              |               | 0.816   |              |               | 0.898   |              |               | 1.000   |              |               | 0.001*  |
| 0, <i>n</i>          | 56       | 30           | 26            |         | 49           | 7             |         | 51           | 5             |         | 21           | 35            |         |
| 1, <i>n</i>          | 78       | 39           | 39            |         | 70           | 8             |         | 70           | 8             |         | 53           | 25            |         |
| Smoking status       |          |              |               | 0.190   |              |               | 0.357   |              |               | 0.877   |              |               | 0.206   |
| Non-smoker, <i>n</i> | 106      | 51           | 55            |         | 96           | 10            |         | 95           | 11            |         | 62           | 44            |         |

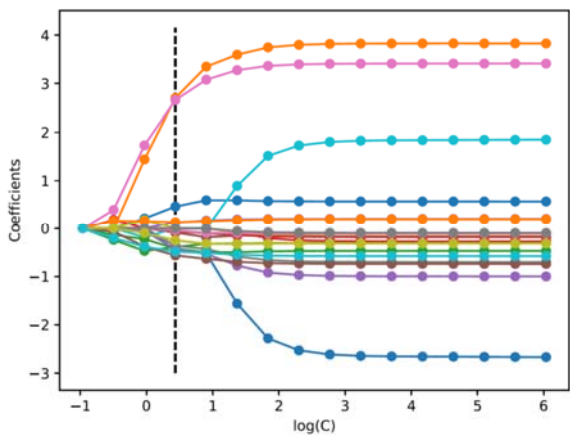
|                             |    |    |    |       |   |       |   |       |       |
|-----------------------------|----|----|----|-------|---|-------|---|-------|-------|
| Smoker, <i>n</i>            | 28 | 18 | 10 | 23    | 5 | 26    | 2 | 12    | 16    |
| Lesion location             |    |    |    | 0.270 |   | 0.362 |   | 0.485 | 0.210 |
| Left upper lobe, <i>n</i>   | 36 | 21 | 15 | 29    | 7 | 33    | 3 | 24    | 12    |
| Left lower lobe, <i>n</i>   | 24 | 9  | 15 | 23    | 1 | 23    | 1 | 14    | 10    |
| Right upper lobe, <i>n</i>  | 39 | 23 | 16 | 36    | 3 | 35    | 4 | 21    | 18    |
| Right middle lobe, <i>n</i> | 6  | 4  | 2  | 5     | 1 | 6     | 0 | 4     | 2     |
| Right lower lobe, <i>n</i>  | 29 | 12 | 17 | 26    | 3 | 24    | 5 | 11    | 18    |

Note. P value indicates the significance between the wildtype and mutation by Wilcox rank sum test.

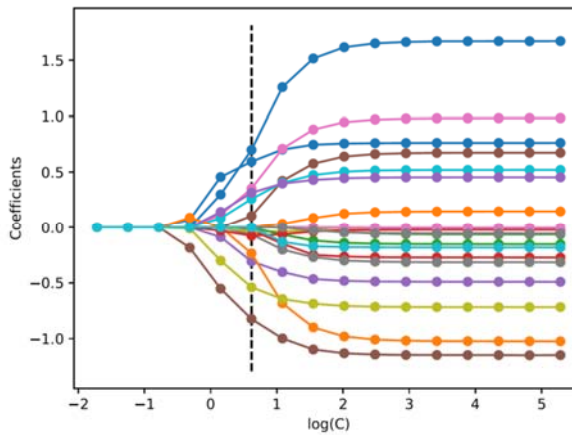
*EGFR*= epidermal growth factor receptor; *KRAS*= Kirsten rat sarcoma viral oncogene; *ERBB2*= Erb-B2 receptor tyrosine kinase 2; *TP53*= tumor protein 53.

**Figure S1.** Logistic regression paths showing the coefficients of top 20 features (13 for *KRAS*) at different lambda values in the least absolute shrinkage and selection operator (LASSO) feature selection procedure. The coefficient profile plots are performed against the log(lambda) sequence. The dotted line shows the feature coefficient at the best lambda value for each mutation status. The coefficient of individual feature is represented by colored line.

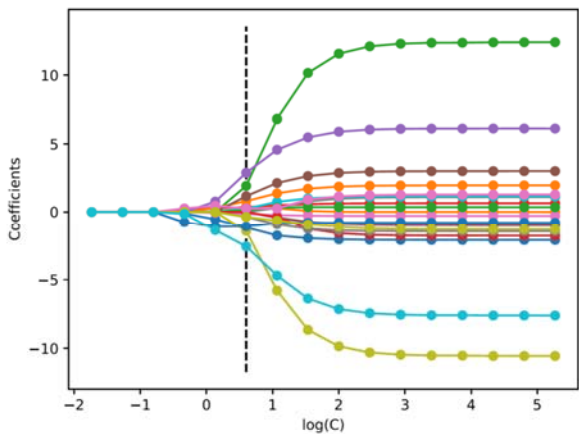
A) Epidermal growth factor receptor (*EGFR*)



B) Kirsten rat sarcoma viral oncogene (*KRAS*)



C) Erb-B2 receptor tyrosine kinase 2 (*ERBB2*)



D) Tumor protein 53 (*TP53*)

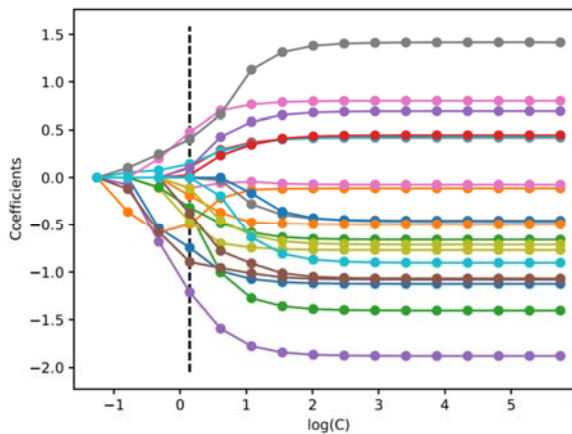
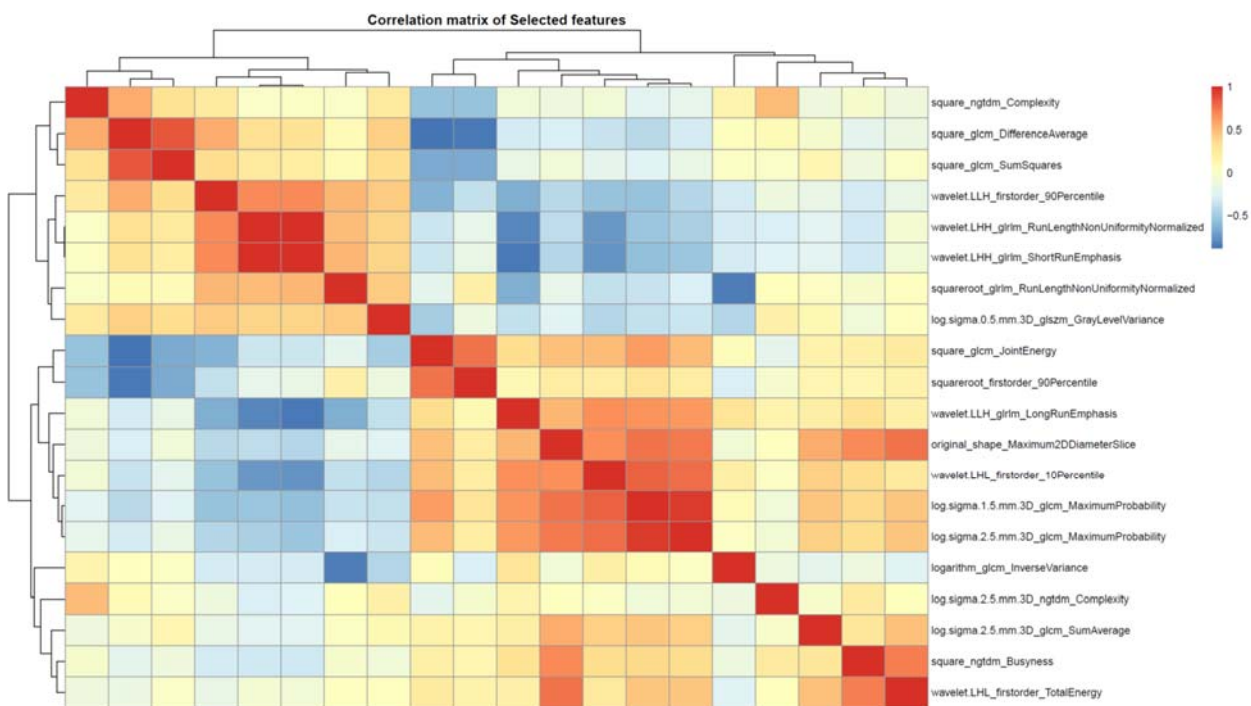


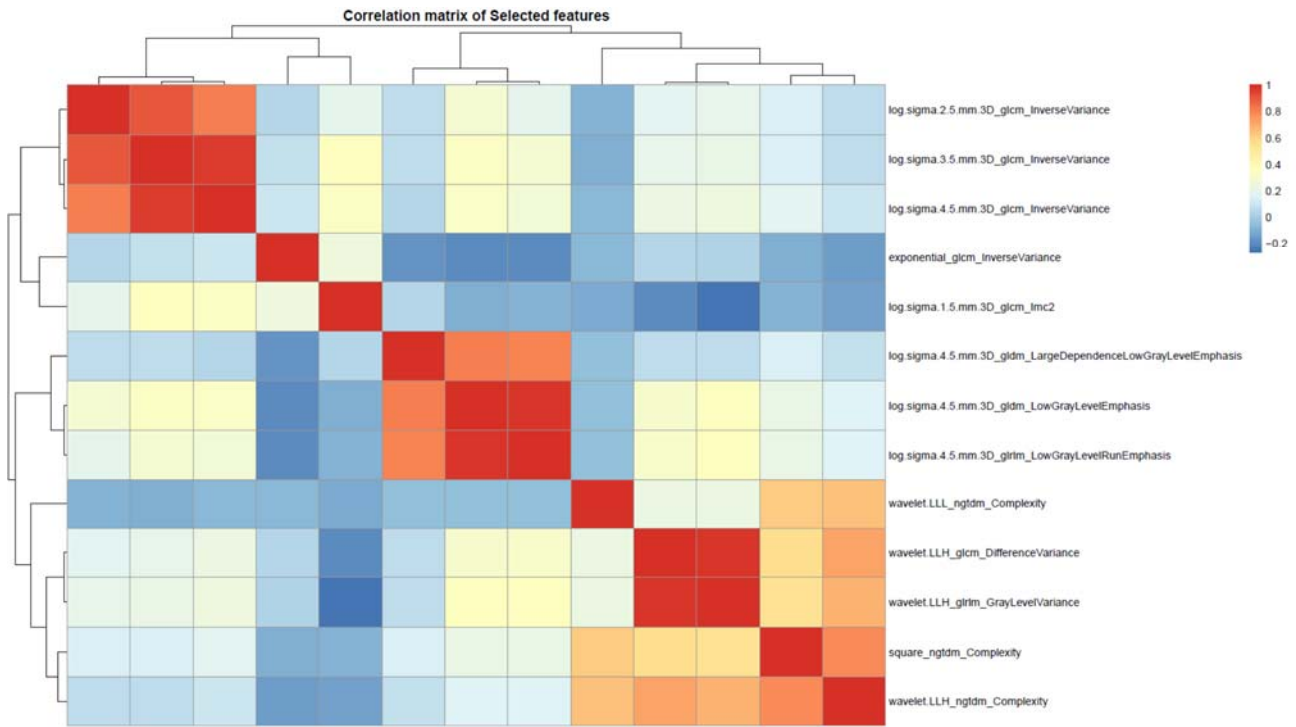


**Figure S2.** Correlation heatmaps with clustering of the most relevant radiomic features with the presence of genetic mutation. The color bar represents the Pearson's correlation coefficient ( $\rho$ ) between the features. The elements of the heatmap are color coded according to the Pearson's correlation coefficient between the features. Red color indicates that the two features are fully positive correlation, and blue color indicates complete negative correlation. The hierarchical cluster dendrogram is also shown in the figure. The top or bottom side of the correlation matrix square represents the most relevant features, and the feature from left to right horizontally is consistent with that from top to bottom vertically.

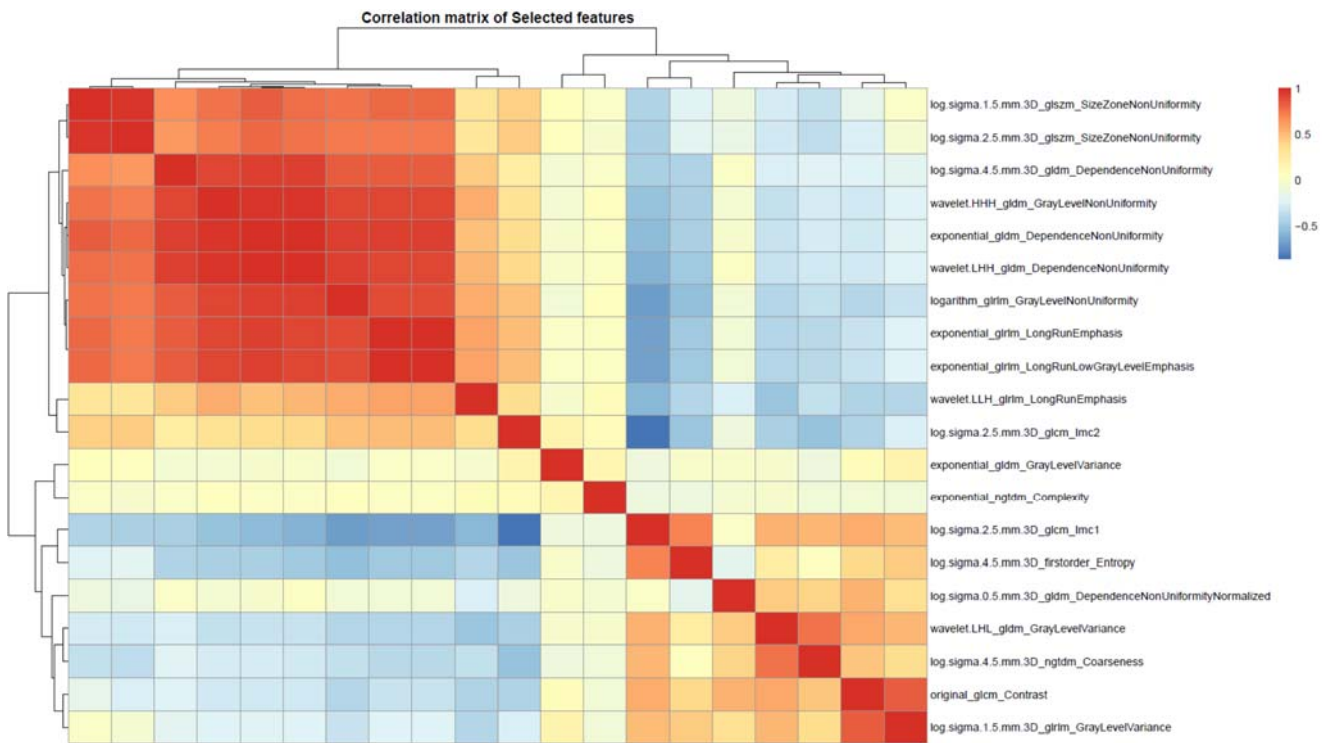
A) Epidermal growth factor receptor (*EGFR*)



B) Kirsten rat sarcoma viral oncogene (*KRAS*)



C) Erb-B2 receptor tyrosine kinase 2 (*ERBB2*)



D) Tumor protein 53 (*TP53*)

Correlation matrix of Selected features

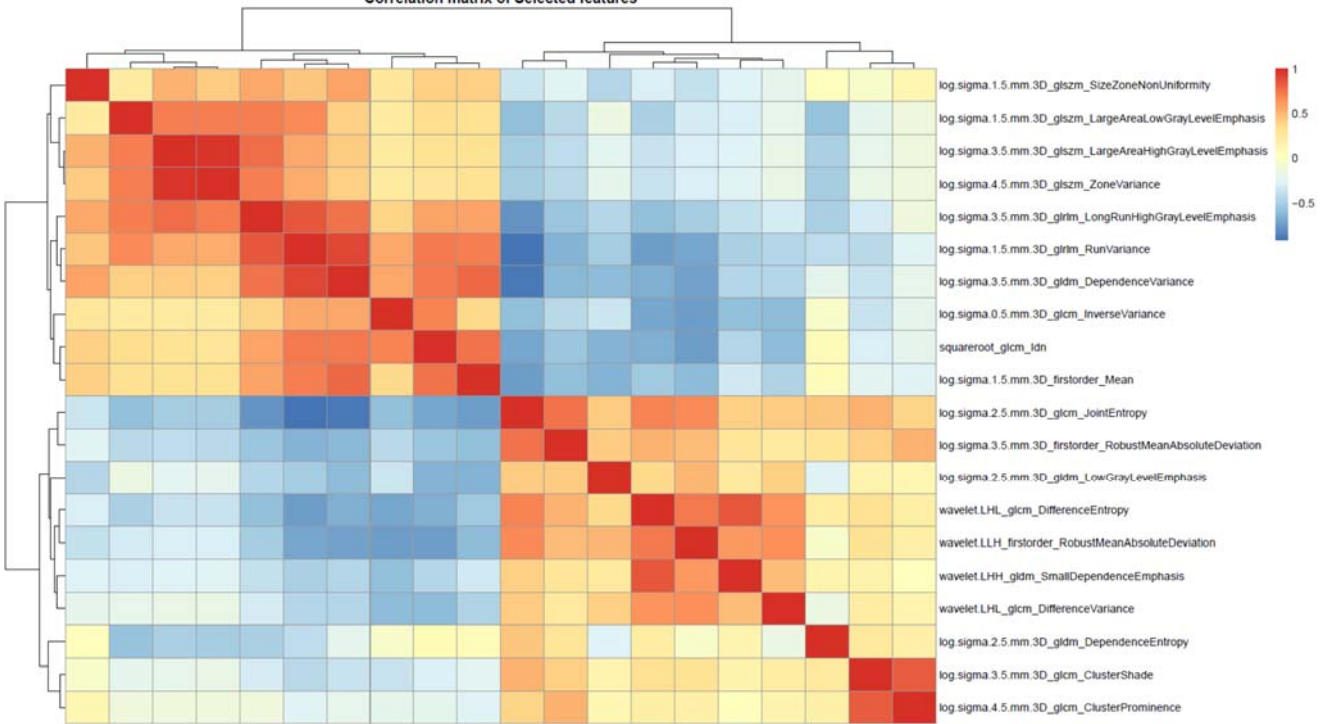
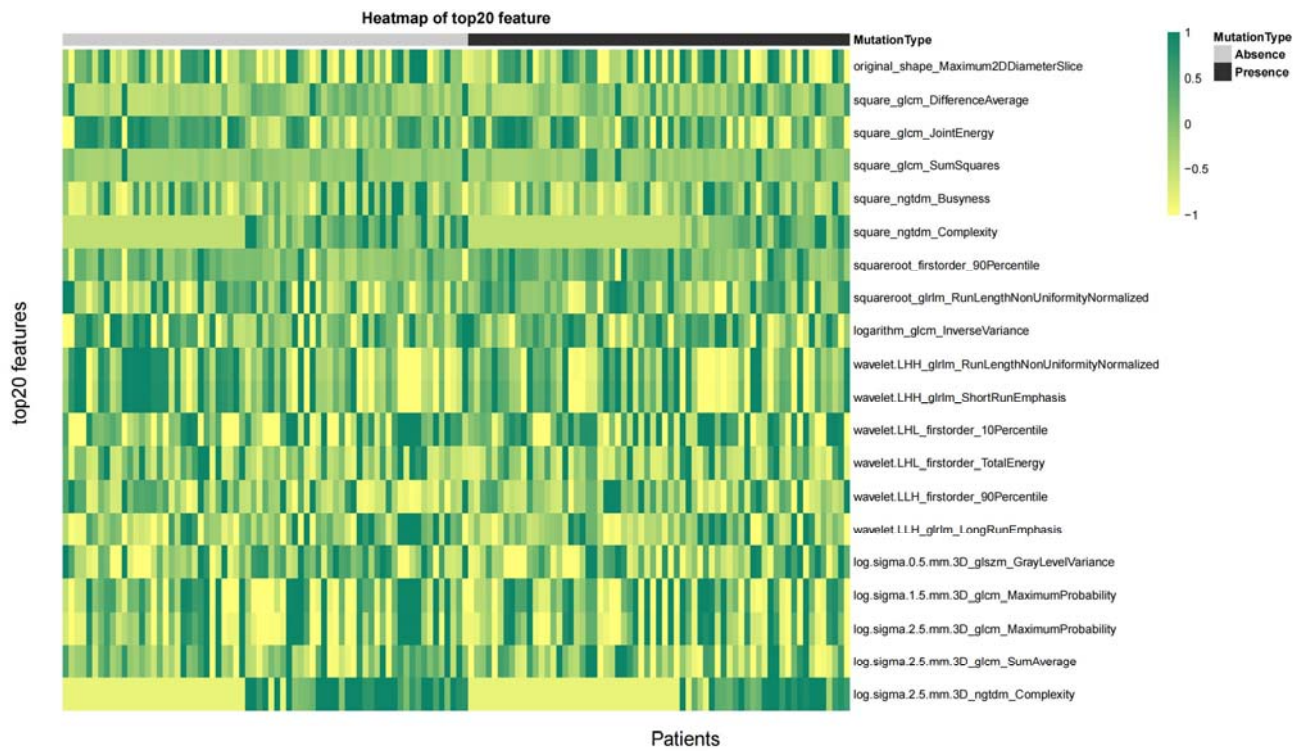
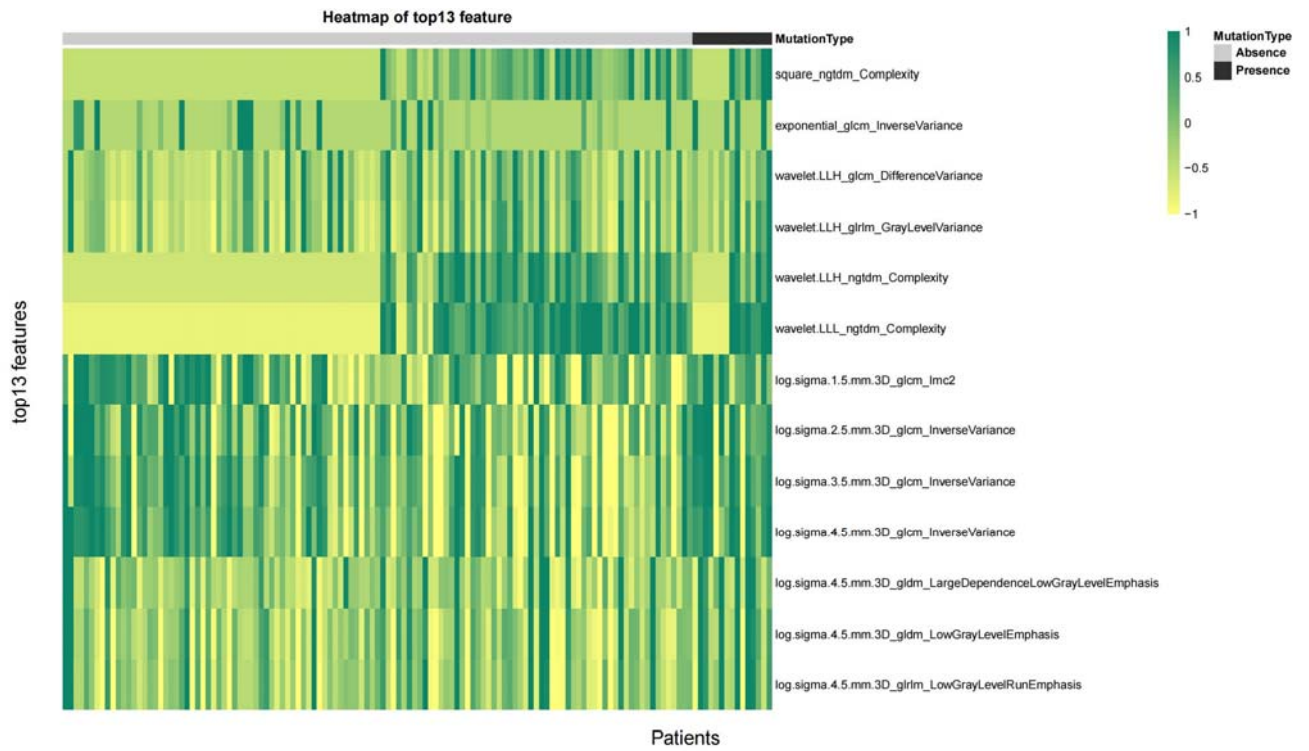


**Figure S3.** Heatmaps of the most relevant radiomic features with the presence of genetic mutation. The color bar represents the normalized values for all features. The elements of the heat map are color coded according to the normalized feature values. Green color represents a larger value and yellow represents a smaller value.

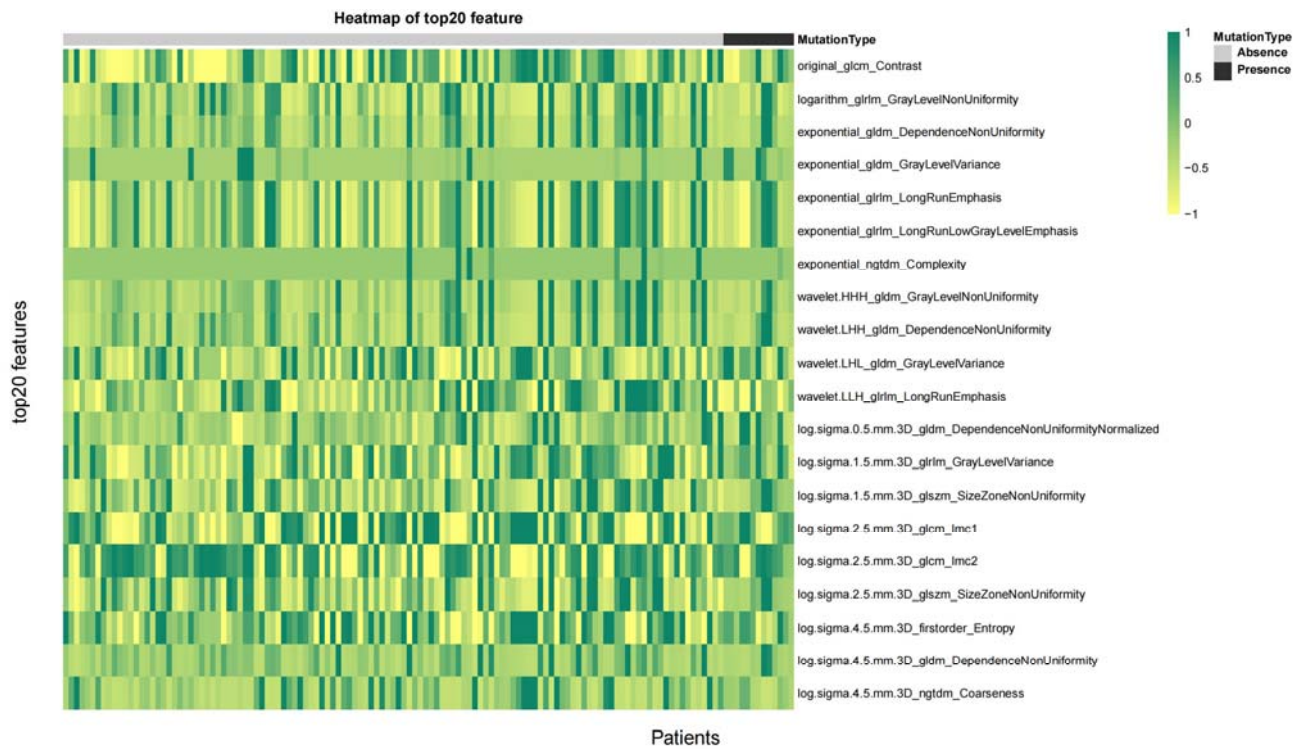
A) Epidermal growth factor receptor (*EGFR*)



B) Kirsten rat sarcoma viral oncogene (*KRAS*)



C) Erb-B2 receptor tyrosine kinase 2 (*ERBB2*)



## D) Tumor protein 53 (*TP53*)

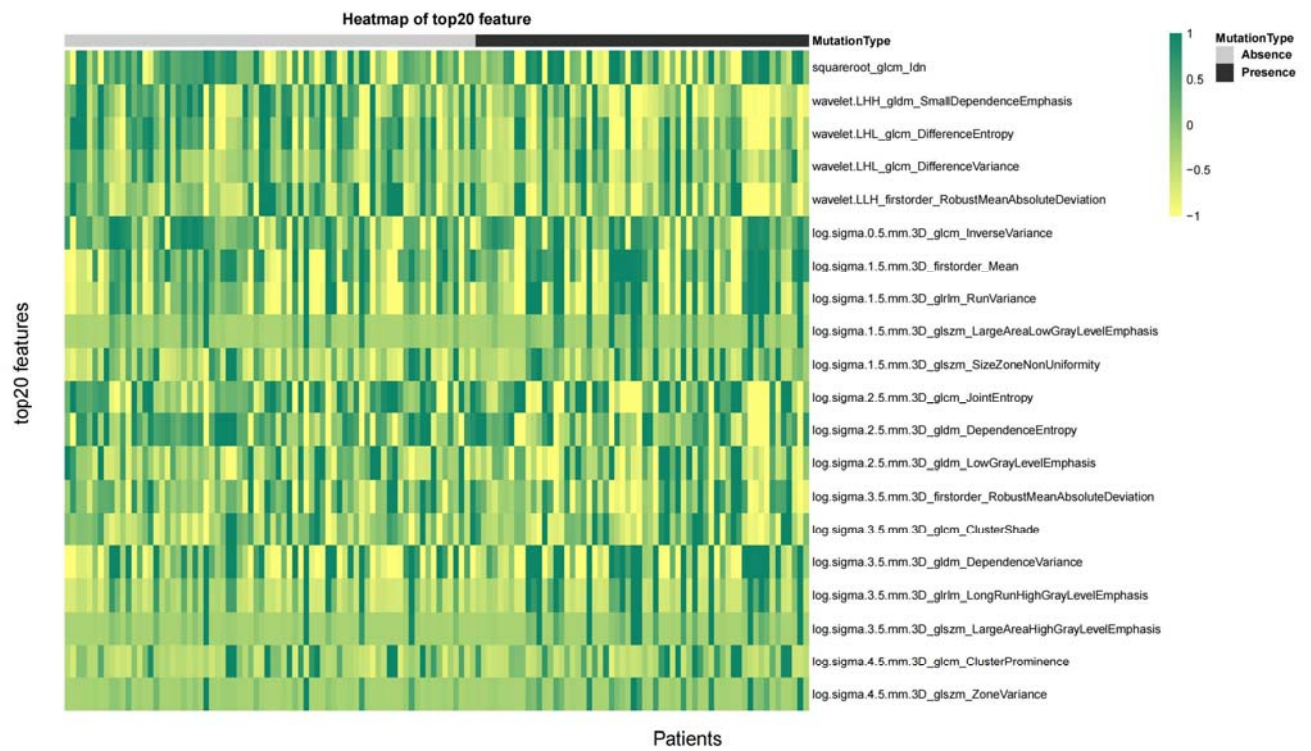
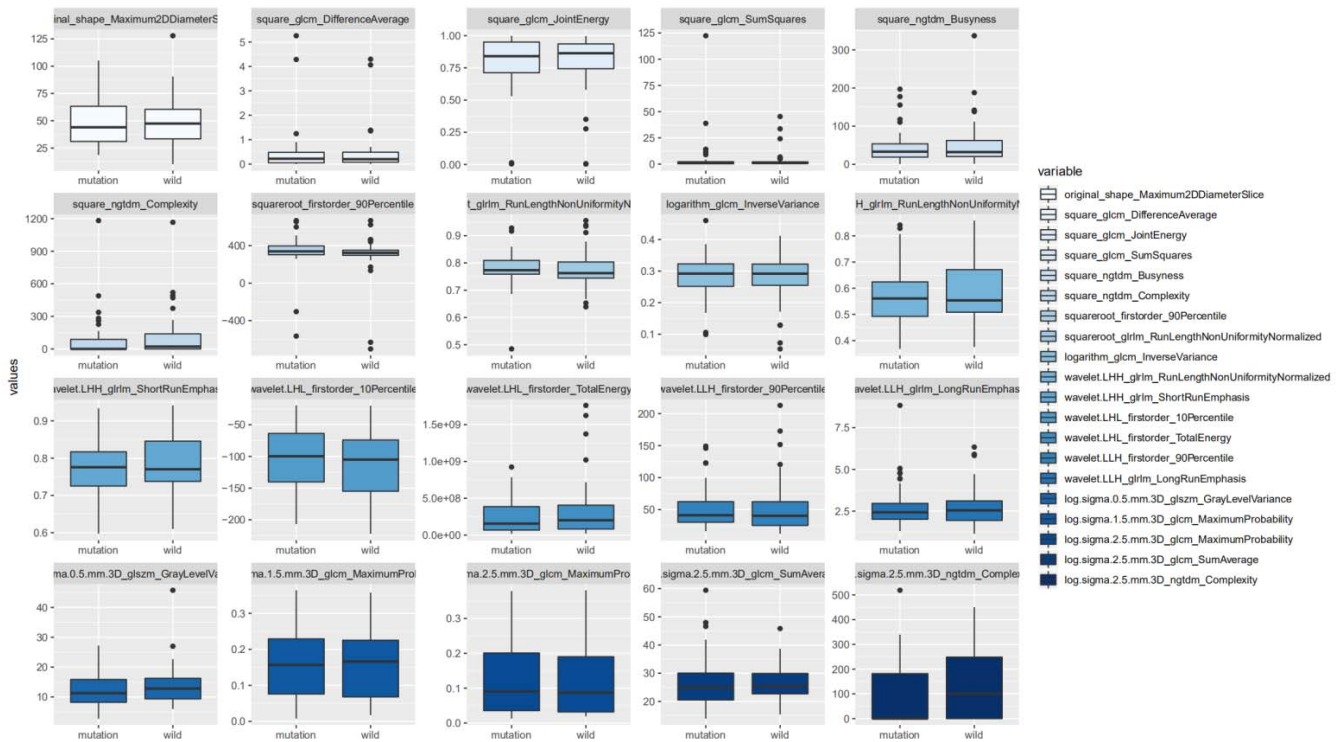
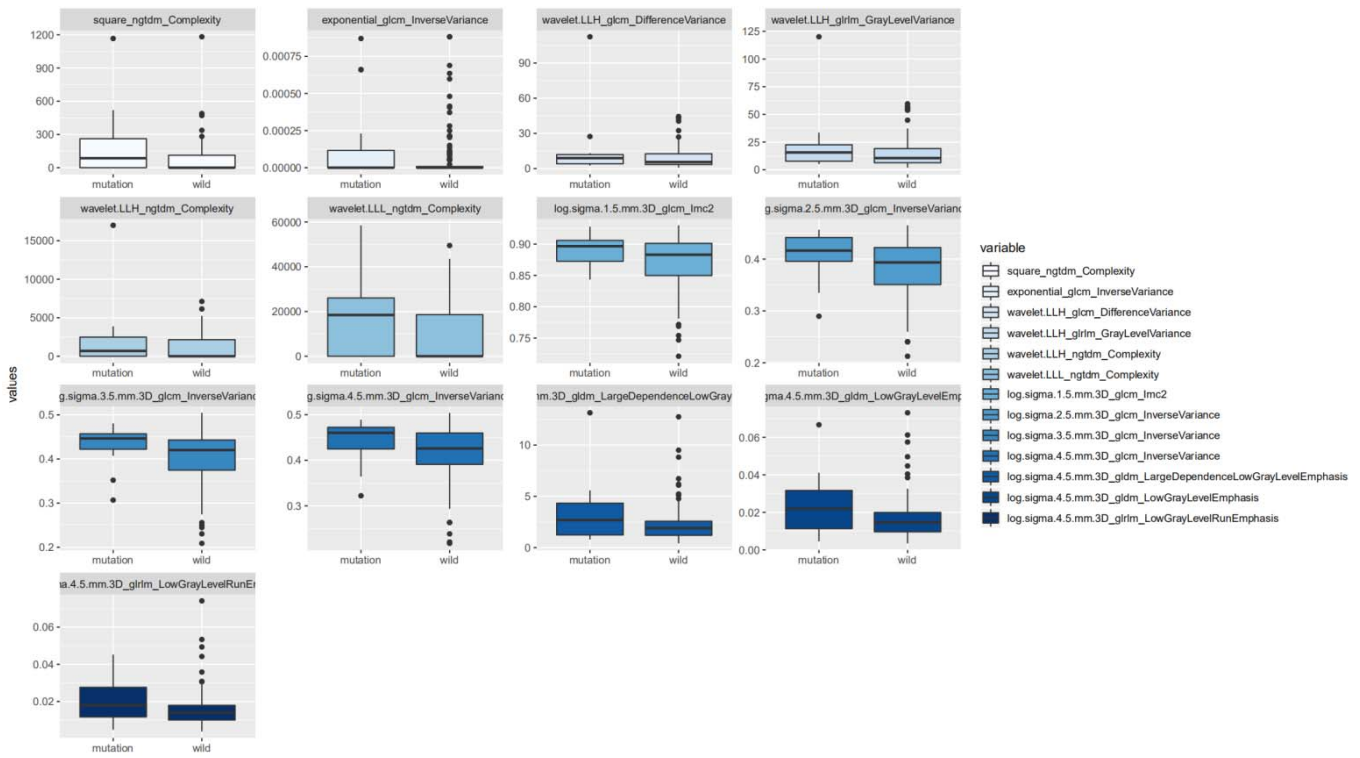


**Figure S4.** Boxplots of the most relevant radiomic features with the presence of genetic mutation

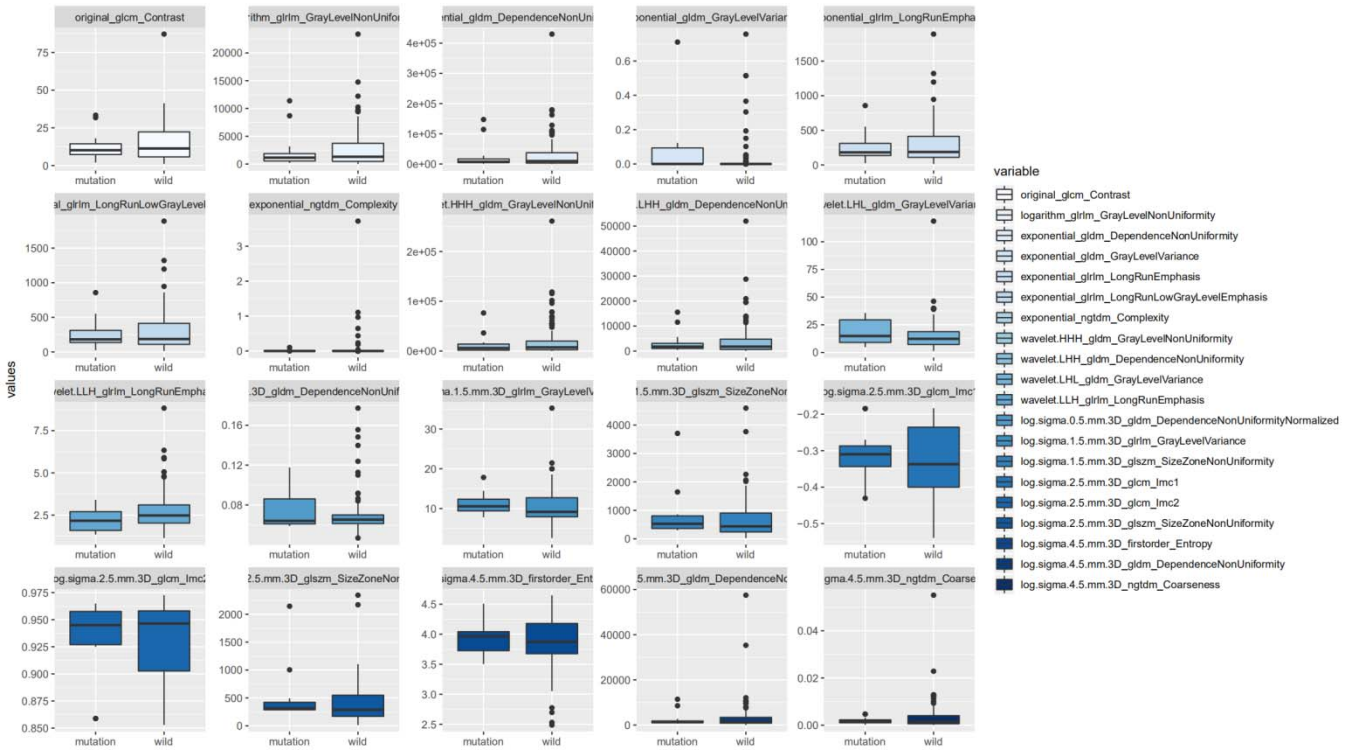
**A) Epidermal growth factor receptor (*EGFR*)**



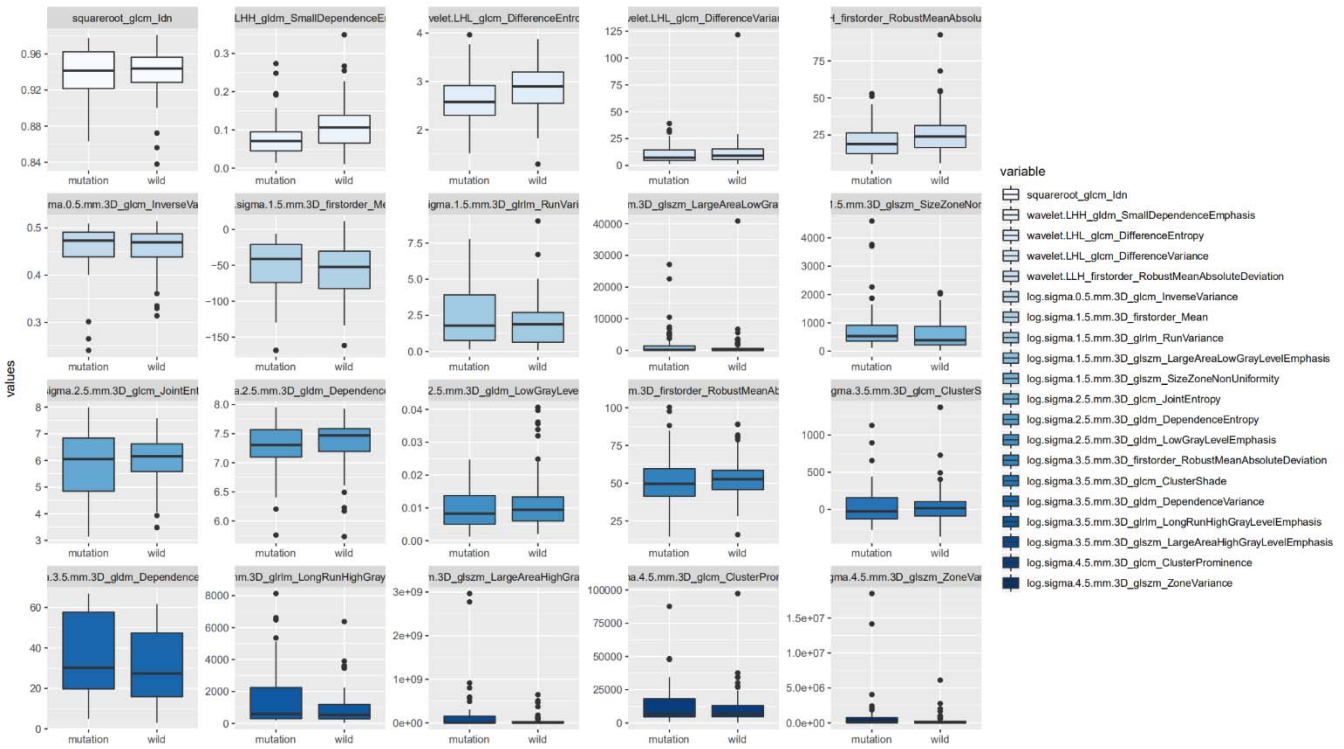
**B) Kirsten rat sarcoma viral oncogene (*KRAS*)**



**C) Erb-B2 receptor tyrosine kinase 2 (*ERBB2*)**



#### D) Tumor protein 53 (*TP53*)





## Supplemental materials

### Radiomic feature interpretation:

#### 1. original\_shape\_Maximum 2D Diameter Slice (Maximum 2D diameter)

Maximum diameter is defined as the largest pairwise Euclidean distance between tumor surface mesh vertices.

#### 2. square\_glcm\_Difference Average

$$\text{Difference average} = \sum_{k=0}^{N_g-1} k p_{x-y}(k)$$

Difference Average measures the relationship between occurrences of pairs with similar intensity values and occurrences of pairs with differing intensity values.

#### 3. square\_glcm\_Joint Energy

$$\text{Joint energy} = \sum_{i=1}^{N_g} \sum_{j=1}^{N_g} (p(i, j))^2$$

Energy is a measure of homogeneous patterns in the image. A greater Energy implies that there are more instances of intensity value pairs in the image that neighbor each other at higher frequencies.

#### 4. square\_glcm\_Sum Squares

$$\text{Sum squares} = \sum_{i=1}^{N_g} \sum_{j=1}^{N_g} (i - u_x)^2 p(i, j)$$

Sum of Squares or Variance is a measure in the distribution of neighboring intensity level pairs about the mean intensity level in the GLCM.

#### 5. square\_ngtdm\_Busyness

$$\text{Busyness} = \frac{\sum_{i=1}^{N_g} p_i s_i}{\sum_{i=1}^{N_g} \sum_{j=1}^{N_g} |ip_i - jp_j|}, \text{ where } p_i \neq 0, p_j \neq 0$$

A measure of the change from a pixel to its neighbour. A high value for busyness indicates a 'busy' image, with rapid changes of intensity between pixels and its neighbourhood.

N.B. if  $N_{g,p} = 1$ , then busyness =  $\frac{0}{0}$ . If this is the case, 0 is returned, as it concerns a fully homogeneous region.

#### 6. square\_ngtdm\_Complexity/log.sigma.2.5.mm.3D\_ngtdm\_Complexity/exponential\_ngtdm\_Complexity

$$\text{Complexity} = \frac{1}{N_{v,p}} \sum_{i=1}^{N_g} \sum_{j=1}^{N_g} |i-j| \frac{p_i s_i + p_j s_j}{p_i + p_j}, \text{ where } p_i \neq 0, p_j \neq 0$$

An image is considered complex when there are many primitive components in the image, i.e. the image is non-uniform and there are many rapid changes in gray level intensity.

#### 7. *squareroot\_firstorder\_90Percentile/ wavelet.LLH\_firstorder\_90Percentile*

The 90<sup>th</sup> percentile of X

#### 8. *squareroot\_glrlm\_Run Length Non-Uniformity Normalized / wavelet.LHH\_glrlm\_Run Length Non-Uniformity*

*Normalized (RLNN)*

$$\text{RLNN} = \frac{\sum_{j=1}^{N_r} (\sum_{i=1}^{N_g} P(i, j | \theta))^2}{N_r(\theta)^2}$$

RLNN measures the similarity of run lengths throughout the image, with a lower value indicating more homogeneity among run lengths in the image. This is the normalized version of the RLN formula.

#### 9. *logarithm\_glcmm\_Inverse Variance/log.sigma.0.5.mm.3D\_glcmm\_InverseVariance*

$$\text{Inverse variance} = \sum_{k=1}^{N_g-1} \frac{p_{x-y}(k)}{k^2}$$

Note that  $k=0$  is skipped, as this would result in a division by 0.

#### 10. *wavelet.LHH\_glrlm\_ShortRunEmphasis (SRE)*

$$\text{SRE} = \frac{\sum_{i=1}^{N_g} \sum_{j=1}^{N_r} \frac{P(i, j | \theta)}{j^2}}{N_r(\theta)}$$

SRE is a measure of the distribution of short run lengths, with a greater value indicative of shorter run lengths and more fine textural textures.

#### 11. *wavelet.LHL\_firstorder\_10Percentile*

The 10<sup>th</sup> percentile of X

#### 12. *wavelet.LHL\_firstorder\_Total Energy*

$$\text{total energy} = V_{\text{voxel}} \sum_{i=1}^{N_p} (X(i) + c)^2$$

Here,  $c$  is optional value, defined by `voxelArrayShift`, which shifts the intensities to prevent negative values in  $X$ . This ensures that voxels with the lowest gray values contribute the least to Energy, instead of voxels with gray level intensity closest to 0.

Total Energy is the value of Energy feature scaled by the volume of the voxel in cubic mm.

**13. *wavelet.LLH\_glrIm\_Long Run Emphasis/ exponential\_glrIm\_LongRunEmphasis (LRE)***

$$LRE = \frac{\sum_{i=1}^{N_g} \sum_{j=1}^{N_r} P(i, j | \theta) j^2}{N_r(\theta)}$$

LRE is a measure of the distribution of long run lengths, with a greater value indicative of longer run lengths and more coarse structural textures.

**14. *log.sigma.0.5.mm.3D\_glszm\_GrayLevelVariance / exponential\_gldm\_GrayLevelVariance/ wavelet.LHL\_gldm\_GrayLevelVariance/ log.sigma.1.5.mm.3D\_glrIm\_GrayLevelVariance(GLV)***

$$GLV = \sum_{i=1}^{N_g} \sum_{j=1}^{N_s} p(i, j) (i - u)^2$$

$$u = \sum_{i=1}^{N_g} \sum_{j=1}^{N_s} p(i, j) i$$

Here,

GLV measures the variance in gray level intensities for the zones.

**15. *log.sigma.1.5.mm.3D\_glcm\_Maximum Probability/ log.sigma.2.5.mm.3D\_glcm\_MaximumProbability***

$$\text{maximum probability} = \max(p(i, j))$$

Maximum Probability is occurrences of the most predominant pair of neighboring intensity values.

**16. *log.sigma.2.5.mm.3D\_glcm\_Sum Average***

$$\text{sum average} = \sum_{k=2}^{2N_g} p_{x+y}(k) k$$

Sum Average measures the relationship between occurrences of pairs with lower intensity values and occurrences of pairs with higher intensity values.

**17. *original\_glcm\_Contrast***

$$contrast = \sum_{i=1}^{N_g} \sum_{j=1}^{N_g} (i-j)^2 p(i, j)$$

Contrast is a measure of the local intensity variation, favoring values away from the diagonal ( $i = j$ ). A larger value correlates with a greater disparity in intensity values among neighboring voxels.

**18. *logarithm\_glrIm\_Gray Level Non-Uniformity/ wavelet.HHH\_gldm\_Gray Level Non-Uniformity (GLN)***

$$GLN = \frac{\sum_{i=1}^{N_g} (\sum_{j=1}^{N_r} P(i, j | \theta))^2}{N_r(\theta)}$$

GLN measures the similarity of gray-level intensity values in the image, where a lower GLN value correlates with a greater similarity in intensity values.

**19. *exponential\_gldm\_Dependence Non-Uniformity/wavelet.LHH\_gldm\_Dependence Non-Uniformity/log.sigma.4.5.mm.3D\_gldm\_Dependence Non-Uniformity***

(DN)

$$DN = \frac{\sum_{j=1}^{N_d} (\sum_{i=1}^{N_g} P(i, j))^2}{N_z}$$

Measures the similarity of dependence throughout the image, with a lower value indicating more homogeneity among dependencies in the image.

**20. *exponential\_glrIm\_LongRunLowGrayLevelEmphasis (LRLGLE)***

$$LRLGLE = \frac{\sum_{i=1}^{N_g} \sum_{j=1}^{N_r} \frac{P(i, j | \theta) j^2}{i^2}}{N_r(\theta)}$$

LRLGLRE measures the joint distribution of long run lengths with lower gray-level values.

**21. *log.sigma.0.5.mm.3D\_gldm\_Dependence Non-Uniformity Normalized (DNN)***

$$DNN = \frac{\sum_{j=1}^{N_d} (\sum_{i=1}^{N_g} P(i, j))^2}{N_z^2}$$

Measures the similarity of dependence throughout the image, with a lower value indicating more homogeneity among dependencies in the image. This is the normalized version of the DLN formula.

## 22. *log.sigma.1.5.mm.3D\_glszm\_Size-Zone Non-Uniformity / log.sigma.2.5.mm.3D\_glszm\_Size-Zone Non-Uniformity*

(SZN)

$$SZN = \frac{\sum_{j=1}^{N_s} (\sum_{i=1}^{N_g} P(i, j))^2}{N_z}$$

SZN measures the variability of size zone volumes in the image, with a lower value indicating more homogeneity in size zone volumes.

## 23. *log.sigma.2.5.mm.3D\_glcm\_Imc1(Informational Measure of Correlation 1)*

$$IMC1 = \frac{HXY - HXY1}{\max\{HX, HY\}}$$

IMC1 assesses the correlation between the probability distributions of ii and jj (quantifying the complexity of the texture), using mutual information  $I(x, y)$ :

$$\begin{aligned} I(i, j) &= \sum_{i=1}^{N_g} \sum_{j=1}^{N_g} p(i, j) \log_2 \left( \frac{p(i, j)}{p_x(i)p_y(j)} \right) \\ &= \sum_{i=1}^{N_g} \sum_{j=1}^{N_g} p(i, j) (\log_2(p(i, j)) - \log_2(p_x(i)p_y(j))) \\ &= \sum_{i=1}^{N_g} \sum_{j=1}^{N_g} p(i, j) \log_2(p(i, j)) - \sum_{i=1}^{N_g} \sum_{j=1}^{N_g} p(i, j) \log_2(p_x(i)p_y(j)) \\ &= -HXY + HXY1 \end{aligned}$$

However, in this formula, the numerator is defined as  $HXY - HXY1$  (i.e.  $-I(x, y)$ ), and is therefore  $\leq 0$ . This reflects how this feature is defined in the original Haralick paper.

In the case where the distributions are independent, there is no mutual information and the result will therefore be 0.

In the case of uniform distribution with complete dependence, mutual information will be equal to  $\log_2(N_g)$ .

Finally,  $HXY - HXY1$  is divided by the maximum of the 2 marginal entropies, where in the latter case of complete dependence (not necessarily uniform; low complexity) it will result in  $IMC1 = -1$ , as  $HX = HY = I(i, j)$ .

## 24. *log.sigma.2.5.mm.3D\_glcm\_Imc2(Informational Measure of Correlation 2)*

$$IMC2 = \sqrt{1 - e^{-2(HXY2 - HXY)}}$$

IMC2 also assesses the correlation between the probability distributions of i and j (quantifying the complexity of the texture). Of interest is to note that  $HXY1 = HXY2$  and that  $HXY2 - HXY \geq 0$  represents the mutual information of the 2

distributions. Therefore, the range of IMC2 = [0, 1), with 0 representing the case of 2 independent distributions (no mutual information) and the maximum value representing the case of 2 fully dependent and uniform distributions (maximal mutual information, equal to  $\log(N_g)$ ). In this latter case, the maximum value is then equal to

$$\sqrt{1 - e^{-2\log_2(N_g)}}, \text{ approaching } 1.$$

#### 25. *log.sigma.4.5.mm.3D\_firstorder\_Entropy*

$$\text{Entropy} = - \sum_{i=1}^{N_g} p(i) \log_2(p(i) + \epsilon)$$

Here,  $\epsilon$  is an arbitrarily small positive number ( $\approx 2.2 \times 10^{-16}$ ).

Entropy specifies the uncertainty/randomness in the image values. It measures the average amount of information required to encode the image values.

#### 26. *log.sigma.4.5.mm.3D\_ngtdm\_Coarseness*

$$\text{Coarseness} = \frac{1}{\sum_{i=1}^{N_g} p_i s_i}$$

Coarseness is a measure of average difference between the center voxel and its neighbourhood and is an indication of the spatial rate of change. A higher value indicates a lower spatial change rate and a locally more uniform texture.

N.B.  $\sum_{i=1}^{N_g} p_i s_i$  potentially evaluates to 0 (in case of a completely homogeneous image). If this is the case, an arbitrary value of  $10^6$  is returned.

#### 27. *squareroot\_glcm\_Idn(Inverse Difference Normalized)*

$$\text{IDN} = \sum_{k=0}^{N_g-1} \frac{p_{x-y}(k)}{1 + \left(\frac{k}{N_g}\right)}$$

IDN (inverse difference normalized) is another measure of the local homogeneity of an image. Unlike Homogeneity1, IDN normalizes the difference between the neighboring intensity values by dividing over the total number of discrete intensity values.

#### 28. *wavelet.LHH\_gldm\_SmallDependenceEmphasis(SDE)*

$$SDE = \frac{\sum_{i=1}^{N_g} \sum_{j=1}^{N_d} \frac{P(i, j)}{i^2}}{N_z}$$

A measure of the distribution of large dependencies, with a greater value indicative of larger dependence and more homogeneous textures.

### 29. *wavelet.LHL\_glcm\_Difference Entropy*

$$\text{Difference entropy} = \sum_{k=0}^{N_g-1} p_{x-y}(k) \log_2(p_{x-y}(k) + \varepsilon)$$

Difference Entropy is a measure of the randomness/variability in neighborhood intensity value differences.

### 30. *wavelet.LHL\_glcm\_Difference Variance*

$$\text{difference Variance} = \sum_{k=0}^{N_g-1} (k - DA)^2 p_{x-y}(k)$$

Difference Variance is a measure of heterogeneity that places higher weights on differing intensity level pairs that deviate more from the mean.

### 31. *wavelet.LLH\_firstorder\_Robust Mean Absolute Deviation/ log.sigma.3.5.mm.3D\_firstorder\_RobustMeanAbsoluteDeviation (rMAD)*

$$rMAD = \frac{1}{N_{10-90}} \sum_{i=1}^{N_{10-90}} |X_{10-90}(i) - \bar{X}_{10-90}|$$

Robust Mean Absolute Deviation is the mean distance of all intensity values from the Mean Value calculated on the subset of image array with gray levels in between, or equal to the 10<sup>th</sup> and 90<sup>th</sup> percentile.

### 32. *log.sigma.1.5.mm.3D\_firstorder\_Mean*

$$\text{mean} = \frac{1}{N_p} \sum_{i=1}^{N_p} X(i)$$

The average gray level intensity within the ROI.

### 33. *log.sigma.1.5.mm.3D\_glrIm\_RunVariance (RV)*

$$RV = \sum_{i=1}^{N_g} \sum_{j=1}^{N_r} p(i, j | \theta) (j - u)^2$$

$$\text{Here, } \mathbf{u} = \sum_{i=1}^{N_g} \sum_{j=1}^{N_r} p(i, j | \theta) j$$

RV is a measure of the variance in runs for the run lengths.

### 34. *log.sigma.1.5.mm.3D\_glszm\_Large Area Low Gray Level Emphasis (LALGLE)*

$$LALGLE = \frac{\sum_{i=1}^{N_g} \sum_{j=1}^{N_s} \frac{P(i, j) j^2}{i^2}}{N_z}$$

LALGLE measures the proportion in the image of the joint distribution of larger size zones with lower gray-level values.

### 35. *log.sigma.2.5.mm.3D\_glcm\_Joint Entropy*

$$\text{joint entropy} = - \sum_{i=1}^{N_g} \sum_{j=1}^{N_g} p(i, j) \log_2(p(i, j) + \varepsilon)$$

Joint entropy is a measure of the randomness/variability in neighborhood intensity values.

### 36. *log.sigma.2.5.mm.3D\_gldm\_Dependence Entropy(DE)*

$$\text{dependence entropy} = - \sum_{i=1}^{N_g} \sum_{j=1}^{N_d} p(i, j) \log_2(p(i, j) + \varepsilon)$$

### 37. *log.sigma.2.5.mm.3D\_gldm\_LowGrayLevelEmphasis (LGLE)*

$$LGLLE = \frac{\sum_{i=1}^{N_g} \sum_{j=1}^{N_d} \frac{P(i, j)}{i^2}}{N_z}$$

Measures the distribution of low gray-level values, with a higher value indicating a greater concentration of low gray-level values in the image.

### 38. *log.sigma.3.5.mm.3D\_glcm\_Cluster Shade*

$$\text{Cluster Shade} = \sum_{i=1}^{N_g} \sum_{j=1}^{N_g} (i + j - u_x - u_y)^3 p(i, j)$$

Cluster Shade is a measure of the skewness and uniformity of the GLCM. A higher cluster shade implies greater asymmetry about the mean.

### 39. *log.sigma.3.5.mm.3D\_gldm\_Dependence Variance(DV)*



$$DV = \sum_{i=1}^{N_g} \sum_{j=1}^{N_d} p(i, j)(j-u)^2, \quad \text{where } u = \sum_{i=1}^{N_g} \sum_{j=1}^{N_d} jp(i, j)$$

Measures the variance in dependence size in the image.

**40. log.sigma.3.5.mm.3D\_glrmlm\_Long Run High Gray Level Emphasis(LRHGLE)**

$$LRHGLRE = \frac{\sum_{i=1}^{N_g} \sum_{j=1}^{N_r} P(i, j | \theta) i^2 j^2}{N_r(\theta)}$$

LRHGLRE measures the joint distribution of long run lengths with higher gray-level values.

**41. log.sigma.3.5.mm.3D\_glszm\_Large Area High Gray Level Emphasis(LAHGLE)**

$$LAHGLE = \frac{\sum_{i=1}^{N_g} \sum_{j=1}^{N_s} P(i, j) i^2 j^2}{N_z}$$

LAHGLE measures the proportion in the image of the joint distribution of larger size zones with higher gray-level values.

**42. log.sigma.4.5.mm.3D\_glcm\_Cluster Prominence**

$$\text{Cluster Prominence} = \sum_{i=1}^{N_g} \sum_{j=1}^{N_g} (i + j - u_x - u_y)^4 p(i, j)$$

Cluster Shade is a measure of the skewness and uniformity of the GLCM. A higher cluster shade implies greater asymmetry about the mean.

**43. log.sigma.4.5.mm.3D\_glszm\_Zone Variance (ZV)**

$$ZV = \sum_{i=1}^{N_g} \sum_{j=1}^{N_s} p(i, j)(j-u)^2$$

$$\text{Here, } u = \sum_{i=1}^{N_g} \sum_{j=1}^{N_s} p(i, j)j$$

ZV measures the variance in zone size volumes for the zones.

### *Biological meaning of the most-relevant features with mutations*

The radiomic features with the lowest p values associated with *EGFR*, *KRAS*, *ERBB2* and *TP53* mutations are listed as follows:

#### 1. *EGFR*

a) `exponential_firstorder_MeanAbsoluteDeviation` (mean distance of all intensity values from the mean value of the image array) indicates the dispersion of CT values in the volume of interest (VOI), which may be associated with the heterogeneity of tumor tissue.

b) `logarithm_gldm_LargeDependenceHighGray LevelEmphasis` (measures the joint distribution of large dependence with higher gray-level values) expresses the distribution of high CT value part, which may be associated with the vascularization of tumor.

#### 2. *ERBB2*

a) `square_ngtdm_Complexity` considers an image as complex when there are many primitive components in the image, i.e., the image is non-uniform and there are many rapid changes in gray level intensity. This feature may be associated with the heterogeneity of tumor tissue.

#### 3. *KRAS*

a) `log.sigma.0.5.mm.3D_firstorder_Minimum` indicates the minimum value in VOI, which may be associated with the heterogeneity of tumor tissue.

b) `original_shape_SphericalDisproportion`. Spherical Disproportion is the ratio of the surface area of the tumor region to the surface area of a sphere with the same volume as the tumor region, and by definition, the inverse of Sphericity. Therefore, the value range is spherical disproportion  $\geq 1$ , with a value of 1 indicating a perfect sphere. This feature may associated with the irregular shaped tumor.

c) `log.sigma.0.5.mm.3D_glrIm_ShortRunHighGrayLevelEmphasis` indicates the homogeneity of high CT values, which may associated with the homogeneity of contrast-enhanced tumor tissues.

#### 4. *TP53*

a) `wavelet.LHH_firstorder_Uniformity` indicates homogeneity, which may associated with the homogeneity of tumor tissue.

b) `original_shape_SurfaceArea` indicates surface area, which may associated with tumor size.

c) `log.sigma.4.5.mm.3D_ngtdm_Complexity` also considers an image as complex when there are many primitive components in the image, i.e., the image is non-uniform and there are many rapid changes in gray level intensity. This feature may be associated with the heterogeneity of tumor tissue.